Chinese Herbal Medicines 17 (2025) 94–107

Contents lists available at ScienceDirect

Chinese Herbal Medicines

journal homepage: www.elsevier.com/locate/chmed

Original Article

Paris saponin VII induces Caspase-3/GSDME-dependent pyroptosis in pancreatic ductal adenocarcinoma cells by activating ROS/Bax signaling

Xiaoying Qian [a,b], Yang Liu [b], Wenwen Chen [b], Shuxian Zheng [c], Yunyang Lu [b], Pengcheng Qiu [b], Xisong Ke [a], Haifeng Tang [b,*], Xue Zhang [a,*]

[a] Center for Chemical Biology, Institute of Interdisciplinary Integrative Medicine Research, Shanghai University of Traditional Chinese Medicine, Shanghai 201203, China
[b] Department of Chinese Materia Medica and Natural Medicines, School of Pharmacy, Air Force Medical University, Xi'an 710032, China
[c] School of Pharmacy, Shaanxi University of Chinese Medicine, Xianyang 712046, China

ARTICLE INFO

Article history:
Received 16 February 2024
Revised 14 March 2024
Accepted 7 April 2024
Available online 18 May 2024

Keywords:
Caspase-3
gasdermin E
pancreatic ductal adenocarcinoma
paris saponin VII
pyroptosis
reactive oxygen species

ABSTRACT

Objective: *Paridis Rhizoma* (Chonglou in Chinese), a traditional Chinese herbal medicine, has been shown have strong anti-tumor effects. Paris saponin VII (PSVII), an active constituent isolated from *Paridis Rhizoma*, was demonstrated to significantly suppress the proliferation of BxPC-3 cells in our previous study. Here, we aimed to elucidate the anti-pancreatic ductal adenocarcinoma (PDAC) effect of PSVII and the underlying mechanism.

Methods: Cell viability was determined by CCK-8, colony formation, and cell migration assays. Cell apoptosis and reactive oxygen species (ROS) production were measured by flow cytometry with annexin V/propidine iodide (Annexin V/PI) and 2′,7′-dichlorodihydrofluorescein diacetate (DCFH-DA), respectively. Pyroptosis was evaluated by morphological features, Hoechst 33342/PI staining assay, and release of lactate dehydrogenase (LDH). JC-1 fluorescent dye was employed to measure mitochondrial membrane potential. Western blotting and reverse transcription-quantitative polymerase chain reaction (RT-qPCR) were used to determine the levels of proteins or mRNAs. The effect *in vivo* was assessed by a xenograft tumor model.

Results: PSVII inhibited the viability of PDAC cells (BxPC-3, PANC-1, and Capan-2 cells) and induced gasdermin E (GSDME) cleavage, as well as the simultaneous cleavage of Caspase-3 and poly (ADP-ribose) polymerase 1 (PARP). Knockdown of GSDME shifted PSVII-induced pyroptosis to apoptosis. Additionally, the effect of PSVII was significantly attenuated by Z-Asp(OMe)-Glu(OMe)-Val-Asp(OMe)-fluoromethylketone (Z-DEVD-FMK), on the induction of GSDME-dependent pyroptosis. PSVII also elevated intracellular ROS accumulation and stimulated Bax and Caspase-3/GSDME to conduct pyroptosis in PDAC cells. The ROS scavenger *N*-acetyl cysteine (NAC) suppressed the release of LDH and inhibited Caspase-9, Caspase-3, and GSDME cleavage in PDAC cells, ultimately reversing PSVII-induced pyroptosis. Furthermore, in a xenograft tumor model, PSVII markedly suppressed the growth of PDAC tumors and induced pyroptosis.

Conclusion: These results demonstrated that PSVII exerts therapeutic effects through Caspase-3/GSDME-dependent pyroptosis and may constitute a novel strategy for preventing chemotherapeutic resistance in patients with PDAC in the future.

1. Introduction

The latest cancer statistics reveal that pancreatic carcinoma is the third leading cause of cancer-related death, combining data for both men and women. Mortality rates have increased gradually, by 0.3% per year. Although the overall cancer mortality in the United States has continued to decline through 2021, the incidence of pancreatic cancer remains on the rise (Siegel, Giaquinto, & Jemal, 2024). The characteristics of pancreatic ductal adenocarcinoma (PDAC) include late diagnosis, early metastasis, rapid proliferation, and high chemotherapy resistance. It also has a 5-year overall survival rate of 10%. Moreover, it is estimated that in the next 20 years, PDAC will become the 2nd leading cause of cancer deaths (Mizrahi, Surana, Valle, & Shroff, 2020). Most patients with PDAC are clinical diagnosed at a progressed stage, limiting opportunities for surgical

* Corresponding authors.
E-mail addresses: tanghaifeng71@163.com (H. Tang), xuezhang@shutcm.edu.cn (X. Zhang).

https://doi.org/10.1016/j.chmed.2024.04.004
1674-6384/

treatment. Consequently, chemotherapy remains the primary treatment option. However, many patients with PDAC develop chemotherapy resistance, resulting in poor outcomes. Therefore, there is an urgent need for new therapeutic targets and agents. At present, the first- and second-line chemotherapy drugs used to treat PDAC include oxaliplatin, 5-fluorouracil, capecitabine, among others. Most of these drugs primarily exert their anti-tumor effects by inducing apoptosis, but the objective response rate of these drugs is only about 20%, mainly due to the escape of apoptosis (De Dosso et al., 2021; Mohammad et al., 2015). In recent years, many studies have confirmed that several potential chemotherapeutics can induce pyroptosis, a newly recognized type of programmed cell death (PCD), and may pave the way for new directions in cancer treatment (Hu et al., 2020; Wang et al., 2017; Zhang et al., 2019).

Paris saponin VII (PSVII), an active ingredient derived from the traditional Chinese herbal medicine *Paridis Rhizoma* (known as Chonglou in Chinese, listed in the *Chinese Pharmacopoeia*), has been reported to suppress multiple types of tumors (Fan et al., 2015; He et al., 2021; Qian et al., 2020; Zhang et al., 2014). These findings suggest that PSVII could be a potential drug candidate for treating cancer. Based on our previous finding, PSVII can inhibit the proliferation of BxPC-3 cells, possibly through its involvement in inducing apoptosis and pyroptosis (Liu et al., 2023). However, the *in vivo* effects of PSVII and the underlying mechanism still need to be clarified.

Pyroptosis is characterized by chromatin condensation, cytoplasmic swelling, the formation of pores in the cytomembrane, cellular content release, and cell lysis (Ding et al., 2016; Shi, Gao, & Shao, 2017). Many studies have shown that gasdermin (GSDM) family members, including gasdermin A (GSDMA), gasdermin B (GSDMB), gasdermin C (GSDMC), gasdermin D (GSDMD) and gasdermin E (GSDME/DFNA5), serve as the executors of pyroptosis (Wang et al., 2017). Typically, GSDMs are self-inhibiting and inactive, when activated by Caspases or other upstream regulatory factors, GSDMs are cleaved, releasing their perforated N-terminal (NT) domain. These NT domains cooperate to form pores in the cytomembrane (Zhang et al., 2020). It is initially ascribed that pyroptosis was caused by the proteolysis of GSDMD by Caspase 1/4/5/11 (Chen et al., 2016). Recent findings have shown that GSDME, another gasdermin, can turn Caspase-3-induced apoptosis into pyroptosis (Wang et al., 2017). After the activation of Caspase-3, GSDME is further cleaved by cleaved-caspase-3, liberating its N-terminus, which can aggregate and form pores in the plasma membrane, resulting in membrane expansion, lactate dehydrogenase (LDH) release, and increased uptake of propidium iodide (PI), all of which are characteristics of pyroptosis (Ding et al., 2016). In addition to apoptosis, GSDME-dependent pyroptosis has been proposed as another mechanism through which chemical drugs eliminate cancer cells (Wang et al., 2017). Thus, triggering pyroptosis in cancer cells *via* the Caspase-3/GSDME pathway is also one of the mechanisms by which chemical drugs defeat cancer (Rogers et al., 2017; Yu et al., 2019; Zhang et al., 2019).

In the present study, we further investigated the effect of PSVII on PDAC cells *in vitro*. Additionally, we examined its impact on a PDAC tumor xenograft model *in vivo*. Finally, we demonstrated that the anti-PDAC effect of PSVII was mediated through the induction of Caspase-3/GSDME-dependent cell pyroptosis.

2. Materials and methods

2.1. Chemicals and reagents

PSVII (45.2 mg) (Fig. 1A) was isolated and identified from the rhizomes of *Paris polyphylla* (1.9 kg) in our laboratory (Liu et al., 2023). Gemcitabine was purchased from MeilunBio (Dalian, China; Lot: MB5386). *N*-Acetyl cysteine (NAC) and Z-DEVD-FMK were from MedChemExpress (Shanghai, China; Lot: NAC 235861, Z-DEVD-FMK 264908). Necrostatin-1 (Nec-1) was obtained from Beyotime Biotechnology Co., Ltd. (Shanghai, China; Lot: 010423230712).

2.2. Cell lines and cell culture

PDAC cell lines (BxPC-3, PANC-1, and Capan-2 cells) were obtained from the Cell Bank of the Chinese Academy of Sciences. PANC-1 cells were cultured in Dulbecco's modified Eagle medium (Procell, Wuhan, China), while BxPC-3 and Capan-2 cells were cultured in RPMI 1640 medium (Procell, Wuhan, China). The culture media were supplemented with 10% fetal bovine serum (FBS) (Procell, Wuhan, China), penicillin (100 U/mL), and streptomycin (100 mg/mL; Procell, Wuhan, China). All the cells were incubated at 37 °C with 5% CO_2 (CCL-170 T-8-CU-UV, ESCO, Singapore City, Singapore).

2.3. Cell viability assay

Cell viability was examined by using a CCK-8 assay kit (Elabscience, Wuhan, China). BxPC-3, PANC-1, and Capan-2 cells were inoculated in 96-well plates at a 7×10^3 cells/well density and cultured at 37 °C for 24 h. PSVII was resuspended in DMSO (Solarbio, Beijing, China). The cells were treated with PSVII at the indicated concentrations (0, 1.25, 2.5, 5, 10, 20, 40 or 80 μmol/L) for 24 h or 48 h. With necrostatin-1, the cells were treated with 10 μmol/L necrostatin-1 and 3 μmol/L PSVII for 24 h. With NAC, the cells were treated with 5 mmol/L NAC and 3 μmol/L PSVII for 24 h. Then, to each well, the CCK-8 reagent (10 μL) was added and incubated at 37 °C for 2 h. The optical density was measured at 450 nm with a microplate reader (AMR-100, ALLSHENG, Hangzhou, China), and cell viability was estimated.

2.3.1. Colony formation assay

BxPC-3, PANC-1, and Capan-2 cells were inoculated in 6-well plates at 1×10^3 cells/well. After 24 h, changing the medium to fresh complete medium. The cells were then treated with 0, 1.5, 3, or 6 μmol/L PSVII for 24 h. Afterwards, the medium was changed to fresh medium, and the cells were cultured for two weeks. Colonies were fixed with 4% paraformaldehyde, and then stained with 0.1% crystal violet (LEAGENE Biotechnology, Beijing, China) according to previous demonstration.

2.3.2. Transwell migration assay

PDAC cells were seeded onto Transwell inserts with a polycarbonate (PC) membrane (pore size 8 μm; NEST, Wuxi, Jiangsu) in 24-well plates, and medium supplemented with PSVII (0, 1.5, 3, 6 μmol/L) was added to the lower chambers. After 24 h of incubation, the inserts of the Transwell were removed. Then, the cells were fixed with 4% paraformaldehyde and visualized with 0.1% crystal violet (LEAGENE Biotechnology, Beijing, China). Cells that did not across through the PC membrane were gently wiped with a cotton swab. Cells that migrated across the PC membrane were viewed with an inverted microscope (IX73 + DP74; OLYMPUS, Tokyo, Japan) and ImageJ software (version 2.10).

2.3.3. Scratch wound healing assay

5×10^5 cells were inoculated into a 6-well plate, then cultured for 24 h. The next day, a micropipette tip of 200 μL was utilized to scratch through the cells, after which the cells were rinsed with PBS to remove the scattered cells. The plates were placed in an incubator with 5% CO_2 and incubated with PSVII (0, 1.5, 3, 6 μmol/L). After 0, 24, 48 and 72 h, cell migration was

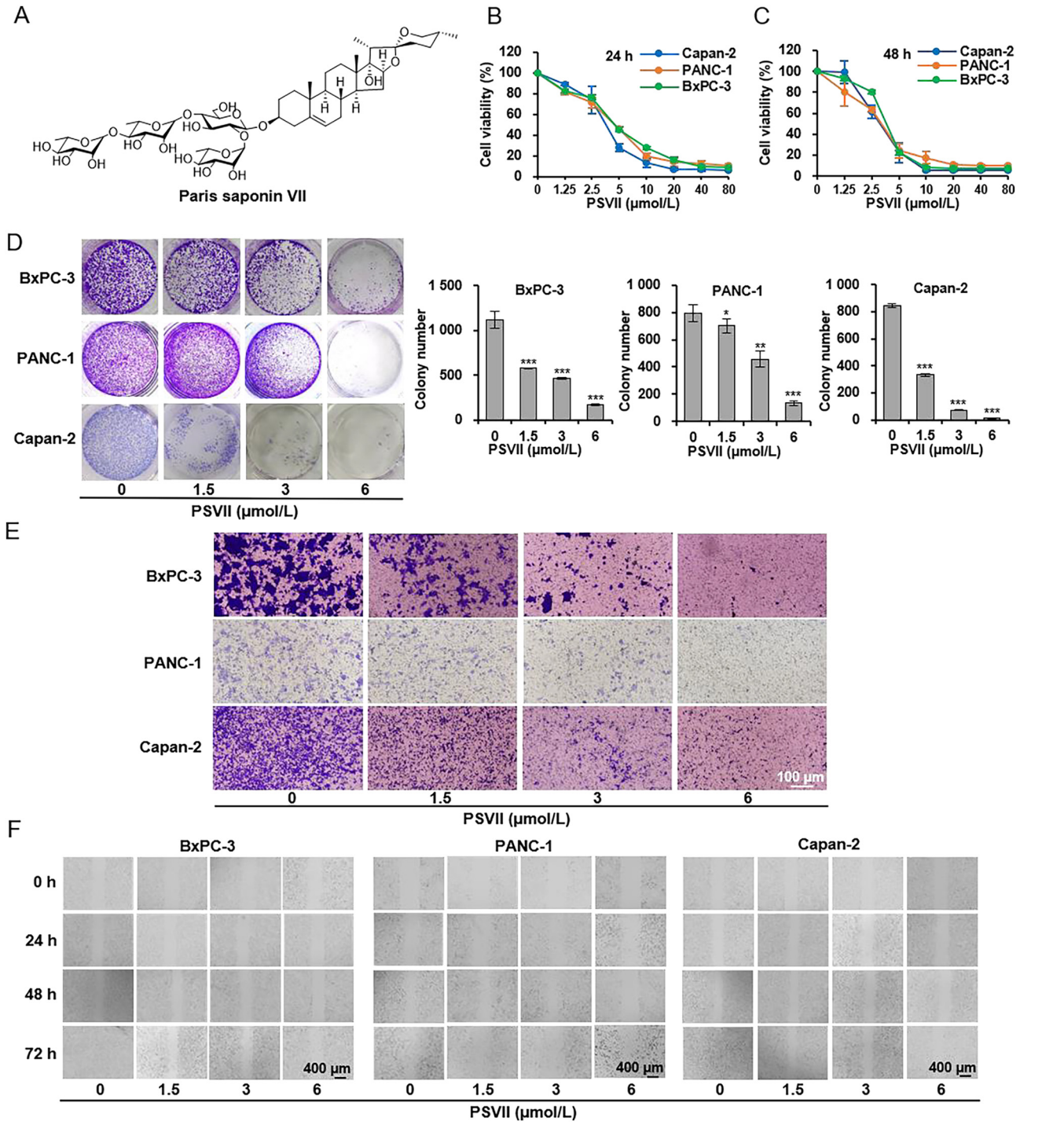

Fig. 1. PSVII inhibited viability and migration of PDAC cells in a concentration-dependent manner. (A) Chemical structure of PSVII. (B and C) BxPC-3, PANC-1, and Capan-2 cells were treated with PSVII for 24 or 48 h, after which cell viability was analyzed. (D) Cells were treated with various concentrations of PSVII (0, 1.5, 3, or 6 μmol/L) for 48 h and then grown for two weeks in fresh medium, colonies were stained with crystal violet and visualized. (E) Migration analysis *via* Transwell assay, scale bar = 100 μm, × 200. (F) Scratch wound healing assay, images of cell scratches were captured at four time points after treatment with various concentrations of PSVII (0, 1.5, 3, or 6 μmol/L), scale bar = 400 μm, × 40. Mean ± SD (n = 3); $^{*}P < 0.05$, $^{**}P < 0.01$, $^{***}P < 0.001$ *vs* control group.

photographed with an inverted microscope (IX73 + DP74; OLYMPUS, Tokyo, Japan).

2.3.4. LDH release assay

PDAC cells were inoculated in 96-well culture plates and administered with PSVII (0, 1.5, 3, 6 μmol/L) for 24 h. With necrostatin-1, the cells were treated with 10 μmol/L necrostatin-1 and 3 μmol/L PSVII for 24 h. With Z-DEVD-FMK, the cells were treated with 20 μmol/L Z-DEVD-FMK and 3 μmol/L PSVII for 24 h. With NAC, the cells were treated with 5 mmol/L NAC and 3 μmol/L PSVII for 24 h. After that, all the supernatant of cell culture was collected, centrifuged at 400 × *g* for 5 min, and analyzed with a LDH detection kit (Beyotime Biotechnology, Shanghai, China). Specifically, 120 μL of supernatant from each well was transferred to a new 96-well plate, after which 60 μL of detection reagent was added. The mixture was incubated at room

temperature (RT) for 30 min in the dark. The OD value was observed at 490 nm. Relative LDH release was calculated as follows: LDH release (%) = (experimental LDH release − medium background) / (maximum LDH release − medium background) × 100.

2.3.5. Hoechst 33342/PI staining assay

A Hoechst 33342/PI staining assay was executed *via* an apoptosis and necrosis assay kit (Beyotime Biotechnology, Shanghai, China). In brief, PDAC cells were cultured in 6-well plate culture dishes (NEST, Wuxi, China) supplemented with PSVII (0, 1.5, 3, 6 μmol/L) for 24 h. Then, Hoechst 33342 and PI were added according to the manufacturer's instructions, and the cells were incubated at 4 °C in the dark for 20 min, and then visualized under an inverted fluorescence microscope (IX73 + DP74; OLYMPUS, Tokyo, Japan).

2.3.6. siRNA transfection

Small interfering RNAs (siRNAs) against GSDMD, GSDME and a negative control (NC) were designed and synthesized by ChemShine Biotechnology (Shanghai, China). Transfection was performed based on the manufacturer's instructions. Lipofectamine 2000 transfection reagent (Invitrogen, Carlsbad, USA) and siRNA were diluted in Opti-MEM medium (Gibco, Carlsbad, USA), respectively. Then, the Opti-MEM medium containing Lipofectamine 2000 was mixed with the Opti-MEM medium containing siRNA, and incubating at RT for 20 min. The cell culture medium was then displaced with the Opti-MEM as described above, after which the cells were cultured for 6 h. The medium was then changed to normal and continued culturing for another 48 h before the following experiments.

2.3.7. Measurement of mitochondrial membrane potential

JC-1 fluorescent dye (Beyotime Biotechnology, Shanghai, China) was applied to measure the mitochondrial membrane potential (MMP) in BxPC-3 cells. The cells were cultured in 6-well culture plates, treated with PSVII, after 24 h incubation, cells were collected and incubated with JC-1 staining solution for 20 min at 37 °C. The MMP was observed with a flow cytometer (Beckman Coulter, Coulter-XL, Brea, USA), and the data were analyzed with EXPO32 ADC Analysis software.

2.3.8. Detection of ROS production and apoptosis by flow cytometry

BxPC-3 cells were inoculated in a 6-well plate, after which the cells were treated with 5 mmol/L NAC and/or 3 μmol/L PSVII for 24 h. The harvested cells were then rinsed twice with PBS and probed with 2′,7′-dichlorodihydrofluorescein diacetate (DCFH-DA) (Beyotime Biotechnology, Shanghai, China) based on the instructions. After that, cells were analyzed by flow cytometry (Beckman Coulter, Coulter-XL, Brea, USA) to detect ROS production. BxPC-3 cells were inoculated and treated as indicated, then harvested, rinsed twice with PBS and probed with an Annexin V-FITC/PI kit (Beyotime Biotechnology, Shanghai, China) in accordance with the instructions. Thereafter, cells were analyzed (Beckman Coulter, Coulter-XL, Brea, USA) to detect apoptosis. The data analyses were applied using EXPO32 ADC Analysis software.

2.3.9. Reverse transcription-quantitative polymerase chain reaction (RT-qPCR)

A RNAsimple total RNA kit (TIANGEN BIOTECH, Beijing, China) was used to extract the total cellular RNA from PDAC cells. Total RNA was subsequently reverse transcribed using the PrimeScript RT Master Mix kit (Takara, Kyoto, Japan). Gene expression was quantified *via* SYBR Green PCR Master Mix (Servicebio, Wuhan, China) on an FTC-3000 system (Funglyn Biotech, Toronto, Canada). The gene expression was normalized relative to the corresponding internal GAPDH levels. The sequences of the primers used are presented in Table 1 (AUGCT DNA-SYN Biotechnology, Beijing, China).

2.3.10. Western blotting

For Western blotting, the cells (*in vitro*) or tumor tissues (*in vivo*) (20−40 mg) were washed with cold PBS twice, prepared by a total protein extraction kit (Keygen BioTECH, Nanjing, Jiangsu) and examined *via* Western blotting as follows. Protein concentrations were quantified by using a bicinchoninic acid (BCA) protein detection kit (Elabscience, Wuhan, China). Equal amounts of lysates were separated by 10% or 12% sodium dodecyl sulfate–polyacrylamide gel electrophoresis (SDS-PAGE) and then transferred to PVDF membranes. The membranes were then blocked with 5% skim milk in phosphoric acid buffer containing Tween-20 (0.1%) solution (PBST) for 2 h and incubated overnight at 4 °C with primary antibodies, including antibodies against Caspase-3, Bax, Bcl-2 (1:1 000; Affinity Biosciences, Jiangsu, China); Caspase-9 (1:500; Santa Cruz Biotechnology, OR, USA); PARP, GSDMD (1:1 000; Proteintech, Wuhan, China); GSDME (1:500; Affinity Biosciences, Jiangsu, China); and β-actin (1:5 000; Servicebio, Wuhan, China). After 5 min × 5 times wash with PBST, the membranes were incubated with goat anti-rabbit IgG-HRP (1:10 000; Elabscience, Wuhan, China) or goat anti-mouse IgG-HRP (1:10 000; Proteintech, Wuhan, China). The membranes with secondary antibodies were incubated for 1 h. The immunoresponse bands were identified *via* an enhanced ECL kit (Engibody Biotechnology, DE, USA) and detected using the ChemiDoc™ XRS system (Bio-Rad, Hercules, CA, USA). Western blotting density analysis was conducted *via* Image Lab 5.1 software, and relative protein expression levels were normalized to that of β-actin.

2.3.11. Transmission electron microscopy assay

After intervention with PSVII, the BxPC-3 cells were collected and fixed with glutaraldehyde (2.5%; Servicebio, Wuhan, China) at 4 °C for 24 h. Afterwards, the cells were fixed in 1% osmium tetroxide for 1 h, then embedded and sectioned. The sections were stained with uranyl acetate and lead citrate, then observed *via* a transmission electron microscope (JEM-1400, Japan Electron Optics Laboratory, Tokyo, Japan).

2.4. Animal study

BALB/c nude mice (male, 3–4 weeks old) were supplied by Slack Jingda Experimental Animal Co., Ltd. (Slack Jingda, Changsha, China) and maintained in the Air Force Medical University Animal Center. The animal study was conducted in accordance with the guiding principles for animal experimentation at Air Force Medical University and received approval from the Laboratory Animal Welfare and Ethics Committee of Air Force Medical University (Xi'an, China) with a No. IACUC-20230096.

Approximately 5 × 10^6 BxPC-3 cells were resuspended in 0.1 mL PBS and injected subcutaneously into the right flank of the mice. Considering that saponins are poorly absorbed with a low oral bioavailability, mice were treated with PSVII or gemcitabine *via* intraperitoneal injection. Pilot experiments were

Table 1
Sequences of primers.

Genes	Forward (5′−3′)	Reverse (5′−3′)
GAPDH	AAGGCTGTGGGCAAGGTCATC	GCGTCAAAGGTGGAGGAGTGG
GSDMA	CTGCTGGATGTGCTTGAG	CCTTCACCTTCACCGTCTT
GSDMB	GCCGTTAGAAGCCTTGTT	GTGTCCAGAATGTCCATCAG
GSDMC	AGATGATGATGAACAGAGAACCTT	CATTGGATGAGGCATTGAAGAG
GSDMD	TGTGTCAACCTGTCTATCA	CTGTATCTGCCCATCCAT
GSDME	TTATGACAGCCTACTTCTTG	ACTCCATCATCAGACAGA

executed to determine the appropriate dosage of PSVII for mice, and PSVII suppressed the growth of PDAC tumors markedly at 2.5 mg/kg body weight.

After the BxPC-3 cells were inoculated, the mice were fed normally. Once the average tumor volumes achieved 100 mm^3, the mice were divided into four groups (n = 4 per group) at random and treated as vehicle controls (normal saline with 0.1% DMSO), the PSVII low dose (PSVII L; 1.25 mg/kg), the PSVII high dose (PSVII H; 2.5 mg/kg) and gemcitabine (60 mg/kg), once every two days. Gemcitabine was injected as a positive control. The length and width of the tumors, as well as the body weight of the tumor-bearing mice, were observed once every three days. The tumor volume was calculated as follows: tumor volume (mm^3) = 1/2 × lengt h × $width^2$. At the end of the experiment, the mice were euthanized, and the tumors were removed, weighed, photographed, and analyzed by Western blotting analysis and immunohistochemical study.

The expressions of Caspase-3 and GSDME in tumor tissues were detected *via* immunohistochemistry. Briefly, the paraffin sections were dewaxed in xylene, then gradient hydrated with 100%–75% ethanol and washed three times in distilled water. Subsequently, citric acid solution (pH = 6.0) was added for repair, and the sections were put in the microwave for 10 min. Next, the sections were cooled in the citric acid solution and then rinsed with PBS 5 min × 3 times. Thereafter, 3% H_2O_2 was added, then incubating at RT for 10 min, after which the slice was rinsed with PBS three times. After blocking with 5% blocking serum at RT for 20 min, the sections were incubated with 50 μL of primary antibodies, including Caspase-3 and GSDME at 4 °C for 24 h. The next day, the slice was rinsed three times by PBS, then added with 50 μL secondary antibody and incubated at 37 °C for 30 min. After the sections were rinsed with PBS 5 min × 3 times, 3,3′-diaminobenzidine tetrahydrochloride (DAB) solution was added, and the sections were incubated at RT for 3 min, and rinsed with distilled water immediately. Subsequently, the sections were counterstained with hematoxylin for 3 min and then washed with distilled water. Eventually, the sections were dehydrated and sealed with neutral gum. The images were captured under a fluorescence microscope (Motic BA400 Digital, Xiamen, China).

2.5. Statistical analysis

The results were expressed as the mean ± standard deviation (SD). All the statistical analyses were executed using GraphPad Prism 8 software. The *in vitro* experiments were repeated at least three times. Significance between two groups were performed using the two-tailed Student's *t*-test. Statistical comparisons among three or more groups were tested by One-way ANOVA test. $P < 0.05$ was considered to indicate statistical significance.

3. Results

3.1. Effects of PSVII on viability and migration of PDAC cell

PDAC cell lines (BxPC-3, PANC-1, and Capan-2) were used to investigate the anti-cancer effects of PSVII in PDAC. The cell viability of PDAC cells was significantly inhibited by PSVII treatment for 24 or 48 h in a concentration-dependent manner (Fig. 1B and C), the IC_{50} at 24 h was (5.31 ± 1.83), (4.99 ± 0.57), and (3.60 ± 0.78) μmol/L for the BxPC-3, PANC-1, and Capan-2 cells, respectively. A colony formation assay showed that PSVII substantially reduced the number of colonies formed by BxPC-3, PANC-1, and Capan-2 cells in a concentration- and time-dependent manner (Fig. 1D). Cell transwell migration experiments revealed that PSVII efficiently inhibited the vertical migration of PDAC cells from the upper chamber to the lower chamber (Fig. 1E). The results of cell wound scratch assay shown in Fig. 1F represented that PSVII markedly inhibited the horizontal migration of cells. Taken together, these results revealed that PSVII inhibited the cell viability and migration ability of BxPC-3, PANC-1, and Capan-2 cells in a concentration-dependent manner.

3.2. PSVII altered cellular morphology and cytomembrane permeabilization

The morphology of BxPC-3, PANC-1, and Capan-2 cells was observed after PSVII treatment. PSVII-treated PDAC cells exhibited morphological changes, such as cell swelling, and these changes differed from the typical features of apoptotic cells, instead resembling the characteristic signs of pyroptosis (Fig. 2A). Therefore, LDH release, which indicates cell membrane rupture and leakage of cell contents, was detected in PDAC cells treated with PSVII in a concentration-dependent manner (Fig. 2B). Inverted fluorescence microscopy analysis indicated that PSVII augmented the proportion of PI-positive PDAC cells in a concentration-dependent manner (Fig. 2C). PI is a kind of membrane-impermeable dye, but in cells undergoing pyroptosis, pores are formed in the cell membrane, through which PI can enter cells and stain nuclei (Miao, Rajan, & Aderem, 2011). The higher release of LDH and the increased proportion of PI-positive cells illustrated that pores had formed in the membrane and that PSVII changed the cell membrane permeability of PDAC cells. However, necrotic cells also exhibit membrane disruption, thus, in this study, necrostatin-1 (Nec-1) was applied to distinguish necroptosis from pyroptosis. As can be seen in Fig. 2D and E, Nec-1 had no substantial impact on PSVII-triggered cell death, or the release of LDH. To observe the changes in the structure of the cell membrane, transmission electron microscopy was applied. Images of BxPC-3 cells treated with PSVII revealed cell membrane rupture, further indicating that PSVII induces pyroptosis in PDAC cells (Fig. 2F). These data demonstrated that PSVII triggered cell death by inducing cell membrane permeabilization, which is a remarkable characteristic of pyroptotic cell death.

3.3. GSDME was necessary for PSVII-triggered pyroptosis in PDAC cells

Gasdermin proteins consist of an N-terminal domain and a C-terminal domain, which are connected by a flexible region. The activated caspases can cleave this region and release the N-terminus, which then forms pores in the cell membrane, leading to the induction of pyroptosis (Shi et al., 2015; Wang et al., 2017; Zhang et al., 2020). The expression of gasdermins in BxPC-3, PANC-1, and Capan-2 cells was detected by RT-qPCR. GSDMD and GSDME were detected in PDAC cells (Fig. 3A). GSDMD has been recognized as a substrate of Caspase 1/4/5/11, and these caspases can cleave GSDMD and release its N-terminus to the cell membrane, ultimately inducing pyroptosis (Shi et al., 2015). Although GSDMD was expressed in BxPC-3, PANC-1, and Capan-2 cells, PSVII treatment did not stimulate the cleavage of GSDMD (Fig. 3B). Furthermore, siRNA-mediated knockdown of GSDMD in BxPC-3 cells (Fig. 3C) had no substantial impact on PSVII induced cell death and the releasing of LDH (Fig. 3D and E). Consequently, GSDMD was not considered to be involved in PSVII-triggered cell death in BxPC-3 cells, therefore, GSDME may be essential for this process. To further verify this, BxPC-3 cells were chosen for subsequent research. Additionally, according to THE HUMAN PROTEIN ATLAS database (https://www.proteinatlas.org/ENSG00000105928-GSDME/cell+line#pancreatic_cancer), BxPC-3 cells exhibited higher expression of GSDME than the other two cell lines, which also indicated that it was more representative.

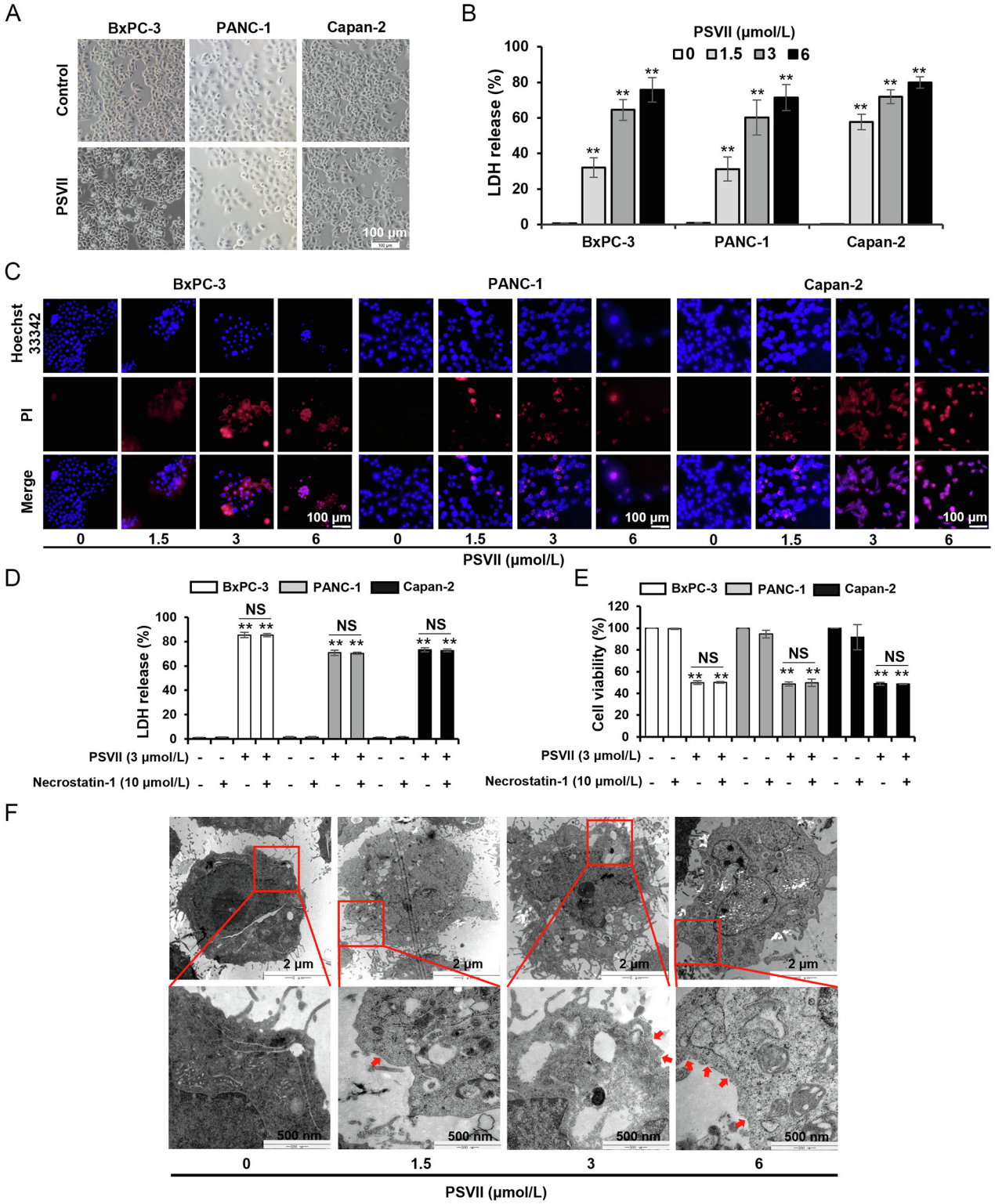

Fig. 2. PSVII triggered pyroptosis in PDAC cells. (A) PDAC cells were treated with PSVII for 24 h, and microscopic imaging was conducted; scale bar = 100 μm, × 100. (B) PDAC cells were treated with various concentrations of PSVII for 24 h, afterwards, LDH release was examined. (C) Hoechst 33342/PI staining assay revealed an increase in number of PI-positive cells (red in the image) after treatment with PSVII; scale bar = 100 μm, × 200. (D and E) PDAC cells were treated with PSVII or necrostatin-1 as indicated, LDH release (D) and cell viability (E) were analyzed. (F) Representative transmission electron microscopy images of BxPC-3 cells treated with PSVII for 24 h were shown, arrowheads indicate cell membrane rupture; scale bars = 2 μm (upper), 500 nm (lower), × 12 000 (upper), × 40 000 (lower). Mean ± SD (n = 3); NS, not significant; $^{**}P < 0.01$ *vs* control group.

3.4. Pyroptosis induced by PSVII in PDAC cells is mediated by GSDME

GSDME exerts anti-tumor effects by mediating pyroptosis in cancer cells and is considered an effective tumor suppressor factor (Zhang et al., 2020). Previous studies have shown that, due to promoter hypermethylation, GSDME is absent or poorly expressed in various types of tumors (Wang et al., 2017). In this study, we found that GSDME was expressed in multiple PDAC cell lines, and Western

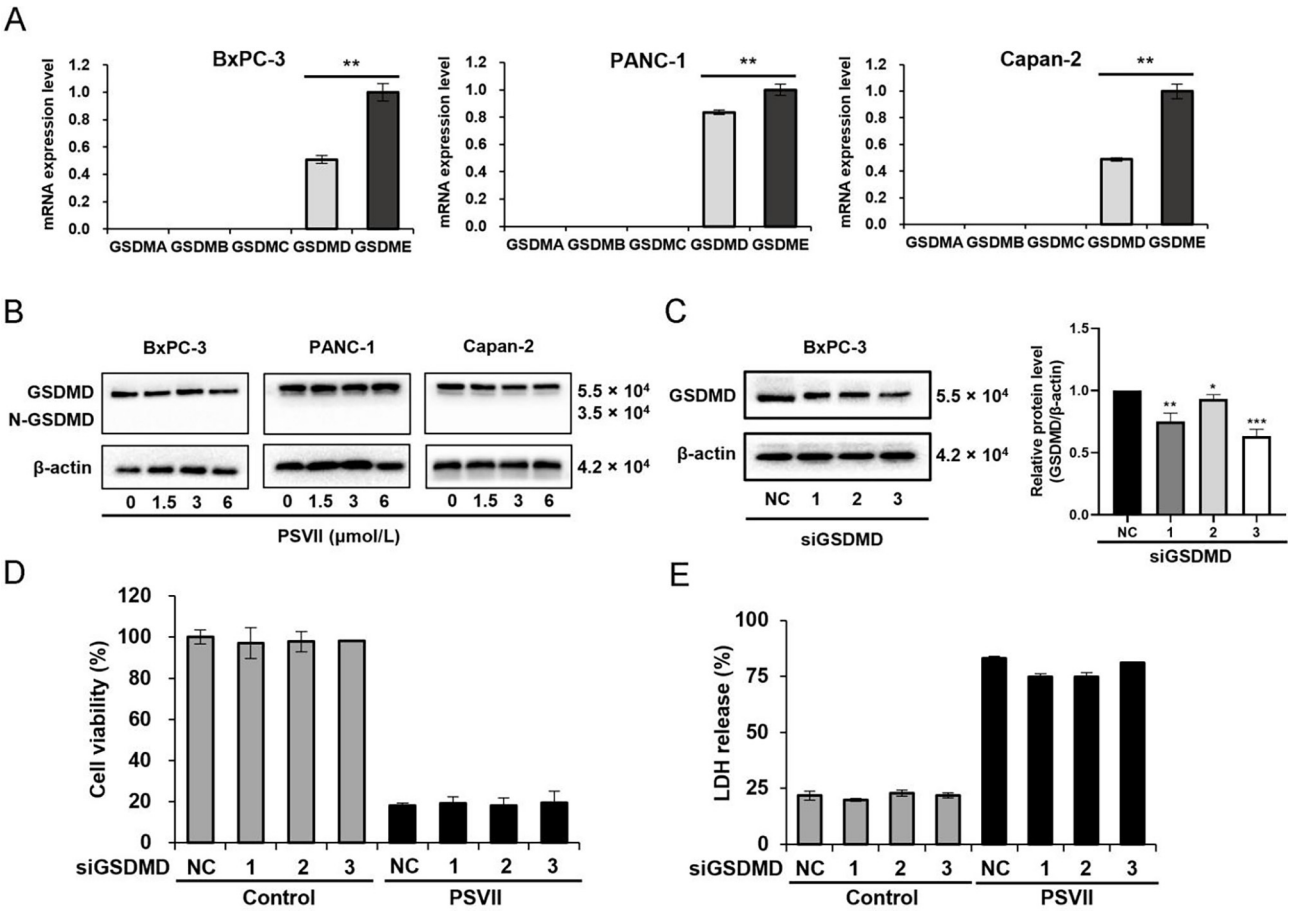

Fig. 3. GSDMD was not associated with PSVII-induced cell death in PDAC cells. (A) mRNA levels of GSDMA, GSDMB, GSDMC, GSDMD, and GSDME were analyzed *via* RT-qPCR. (B) PDAC cells were treated with PSVII (0, 1.5, 3, or 6 μmol/L) for 24 h, afterwards, total cellular extracts were prepared, followed by Western blotting analysis. (C) BxPC-3 cells were transfected with siRNA targeting GSDMD (siGSDMD-1/siGSDMD-2/siGSDMD-3) or a negative control (NC), followed by Western blotting analysis. (D and E) BxPC-3 cells were transfected with GSDMD siRNA-1/-2/-3 or NC siRNA and then treated with PSVII, cell viability (D) and LDH release (E) were analyzed. Mean ± SD (n = 3); $^{*}P < 0.05$, $^{**}P < 0.01$, $^{***}P < 0.001$ *vs* NC group.

blotting results showed that PSVII concentration-dependently cleaved GSDME, Caspase-3, and PARP in BxPC-3 cells (Fig. 4A). To further verify this effect, siRNA technology was used to knock down GSDME in BxPC-3 cells. Western blotting and RT-qPCR analyses confirmed that GSDME expression was effectively reduced in BxPC-3 cells (Fig. 4B and C). Meanwhile, PSVII treated siGSDME cells yielded more cleavage of PARP (Fig. 4D), further confirming that the death mode was switched to apoptosis. Taken together, these findings indicated that in PDAC, PSVII induces pyroptosis through the key regulator GSDME. Furthermore, knocking down GSDME resulted in a remarkable decrease in PSVII evoked LDH release, but the knockdown was unable to reverse the cell death induced by PSVII intervention (Fig. 4E and F). PSVII treated BxPC-3 cells exhibited double-positive stage for Annexin V and PI, indicating the occurrence of pyroptosis. However, the knockdown of GSDME delayed this process, leading to an increase in the percentage of Annexin V-positive cells and a decrease in the proportion of Annexin V/PI double-positive cells, indicating a switch from pyroptosis to apoptosis (Fig. 4G). Taken together, these findings revealed that GSDME was a key protein that was essential for PSVII induced pyroptosis.

3.5. PSVII activated mitochondrial pathway and led to Caspase-3/GSDME-dependent pyroptosis

Recent studies have shown that activation of the mitochondrial apoptotic pathway may induce GSDME-dependent pyroptosis (Rogers et al., 2017). JC-1 is a fluorescent dye that can selectively enter mitochondria. As the membrane potential decreases, the color of the mitochondria changes reversibly from red to green, thus serving as an indicator of changes in the mitochondrial membrane potential (MMP). After BxPC-3 cells were exposed to PSVII, flow cytometry showed an increase in the percentage of green fluorescent cells and a decrease in the percentage of red fluorescent cells, indicating MMP disruption (Fig. 5A). Western blotting was applied to measure the levels of proteins in the mitochondrial intrinsic apoptotic pathway in response to PSVII treatment. PSVII increased Bax and promoted the cleavage of Caspase-9 effectively, while Bcl-2 was downregulated in a concentration-dependent manner, suggesting that PSVII induced pyroptosis in BxPC-3 cells might occur through the mitochondrial apoptotic pathway (Fig. 5B). Subsequently, the Caspase-3-specific inhibitor Z-DEVD-FMK was used, and treatment of cells with a combination of PSVII and Z-DEVD-FMK resulted in a reduction in the cleavage of GSDME and the release of LDH (Fig. 5C and D). Z-DEVD-FMK increased the percentage of Annexin V-positive cells, decreased the proportion of Annexin V/PI double-positive cells among the PSVII treated BxPC-3 cells (Fig. 5E). These findings illustrated that PSVII triggered Caspase-3/GSDME-dependent pyroptosis through activating the mitochondrial apoptotic pathway in PDAC cells.

3.6. PSVII triggered pyroptosis through ROS mediated signaling in PDAC cells

It is indicated that PSVII induces apoptosis and activates the ROS-mediated mitochondrial intrinsic apoptotic pathway in can-

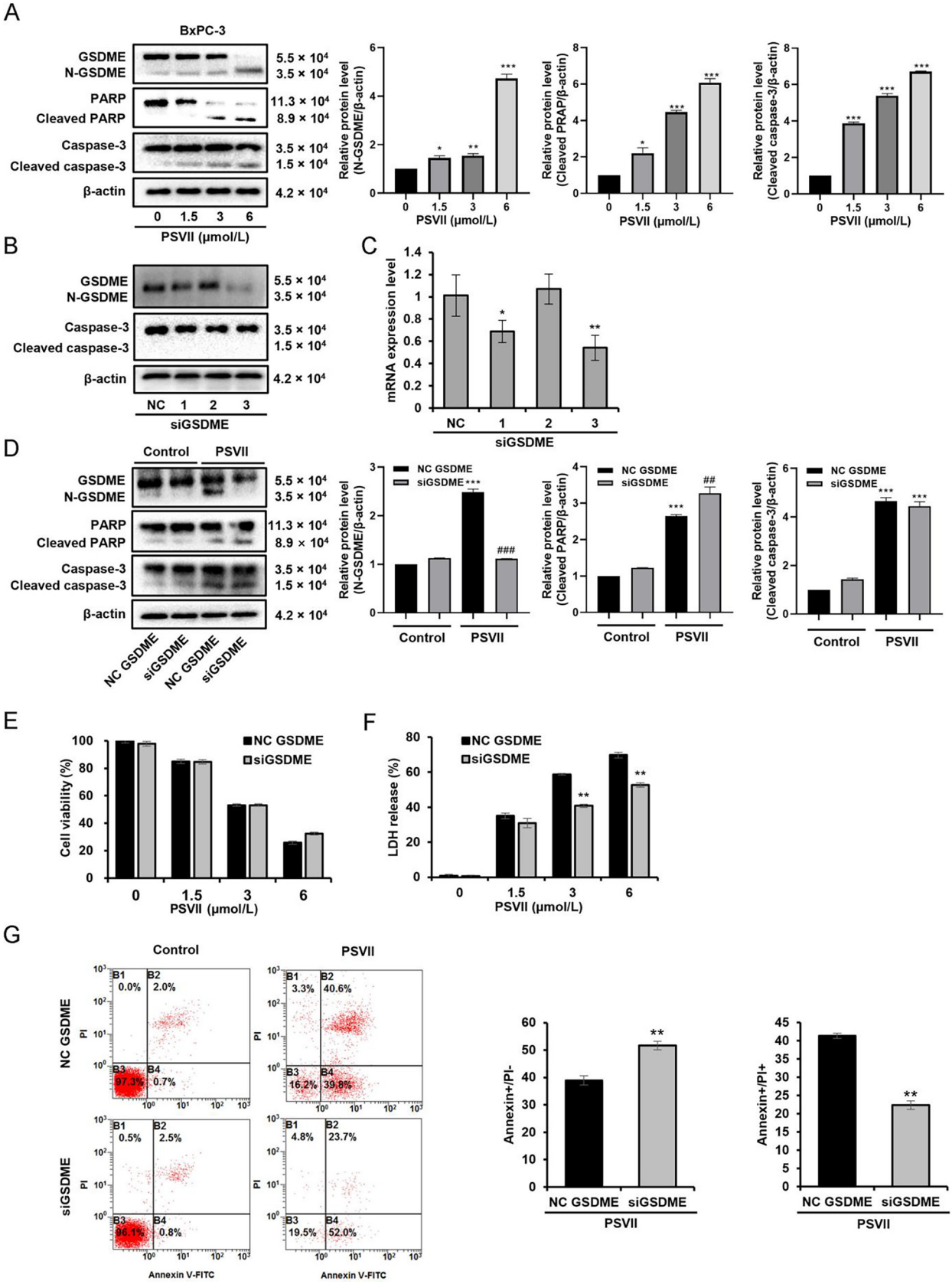

Fig. 4. Pyroptosis induced by PSVII in PDAC cells was mediated by GSDME. (A) BxPC-3 cells were treated with PSVII (0, 1.5, 3, or 6 μmol/L) for 24 h, followed by Western blotting analysis. $^{*}P < 0.05$, $^{**}P < 0.01$, $^{***}P < 0.001$ *vs* control group. (B and C) BxPC-3 cells were transfected with siRNA targeting GSDME (siGSDME-1/siGSDME-2/siGSDME-3) or a negative control (NC), protein levels (B) and mRNA levels (C) were analyzed. $^{*}P < 0.05$, $^{**}P < 0.01$ *vs* NC group. (D) NC GSDME and siGSDME BxPC-3 cells were treated with PSVII (3 μmol/L) for 24 h, followed by Western blotting analysis. $^{***}P < 0.001$ *vs* NC control group, $^{\#\#}P < 0.01$, $^{\#\#\#}P < 0.001$ *vs* NC PSVII-treated group. (E and F) BxPC-3 cells transfected with NC GSDME or siGSDME were treated with PSVII (0, 1.5, 3, or 6 μmol/L) for 24 h, cell viability (E) and LDH release (F) were analyzed, $^{**}P < 0.01$ *vs* NC group. (G) NC GSDME and siGSDME BxPC-3 cells treated with PSVII for 24 h were analyzed by flow cytometry with Annexin V/PI staining. $^{**}P < 0.01$ *vs* NC group. Mean ± SD (n = 3).

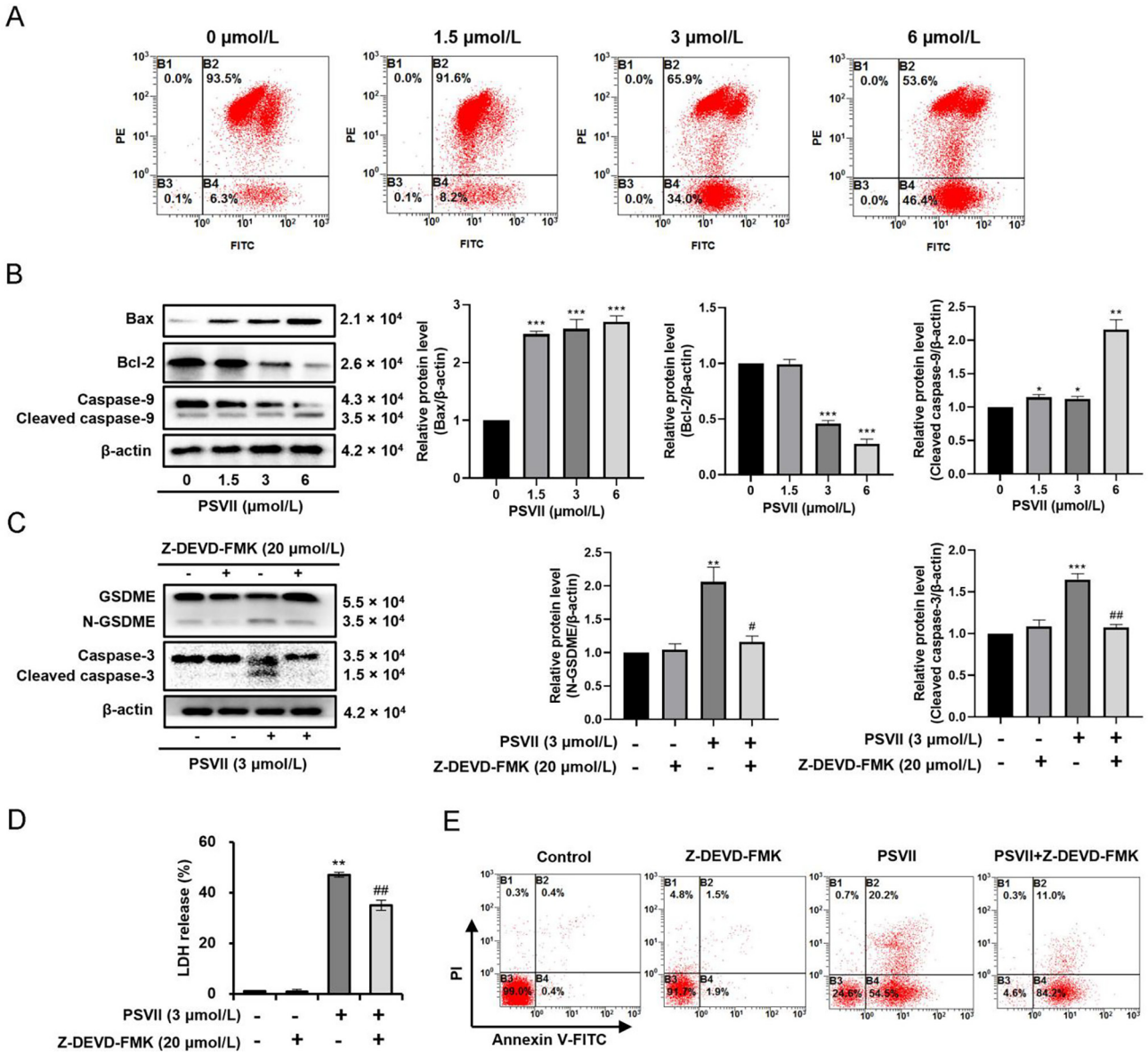

Fig. 5. PSVII activated mitochondrial apoptotic pathway to induce Caspase-3/GSDME-dependent pyroptosis. (A) BxPC-3 cells were treated with PSVII for 24 h, and JC-1-probed cells were analyzed *via* flow cytometry. (B) Total cellular extracts were prepared and then subjected to Western blotting analysis. (C–E) BxPC-3 cells were treated with PSVII in absence or presence of Z-DEVD-FMK (20 μmol/L), followed by Western blotting analysis (C), LDH release assay (D) and flow cytometry with Annexin V-FITC/PI staining (E). Mean ± SD (n = 3); $^{*}P < 0.05$, $^{**}P < 0.01$, $^{***}P < 0.001$ *vs* control group; $^{\#}P < 0.05$, $^{\#\#}P < 0.01$ *vs* PSVII-treated group.

cer cells (Qian et al., 2020; Zhang et al., 2016). However, the relationship between ROS accumulation and cell pyroptosis induced by PSVII is still unknown. Flow cytometry with DCFH-DA was used to determine ROS accumulation, and the results demonstrated that PSVII induced excess ROS production in BxPC-3 cells, which was distinctly abrogated by NAC, a ROS scavenger (Fig. 6A). To assess the function of ROS in PSVII triggered pyroptosis, BxPC-3 cells were pretreated with NAC and then stimulated with PSVII, after which LDH release and cell viability were evaluated. These findings suggested that NAC can decrease the release of LDH and ameliorate PSVII induced cell death (Fig. 6B and C). Moreover, the upregulation of Bax, and the promoted cleavage of Caspase-9, Caspase-3 and GSDME by PSVII were reversed after combined treatment with PSVII and NAC (Fig. 6D and E). These results illustrated that ROS played an essential role in PSVII triggered pyroptosis in PDAC cells.

3.7. PSVII suppressed tumor growth and induced pyroptosis in vivo

The anti-PDAC activity of PSVII *in vivo* was tested by using a BxPC-3 cells subcutaneous xenograft tumor model. Gemcitabine (60 mg/kg) was used as a positive control. PDAC tumor growth was substantially suppressed by gemcitabine and PSVII H treatment. The effects of PSVII H on tumor volume and tumor weight were comparable to those of gemcitabine (Fig. 7A and B). The average weight of the tumors reduced from 673.5 mg (control) to 655.1 mg (PSVII L, 1.25 mg/kg), 437.9 mg (PSVII H, 2.5 mg/kg), and 369.9 mg (gemcitabine, 60 mg/kg), respectively (Fig. 7B). The images of xenograft tumors also suggested that PSVII can reduce the tumor burden *in vivo* (Fig. 7C). Compared to those in the control group, the average body weights of the mice in the PSVII treatment group did not significantly decrease (Fig. 7D). To explore whether the reduction in tumor burden was related to PSVII

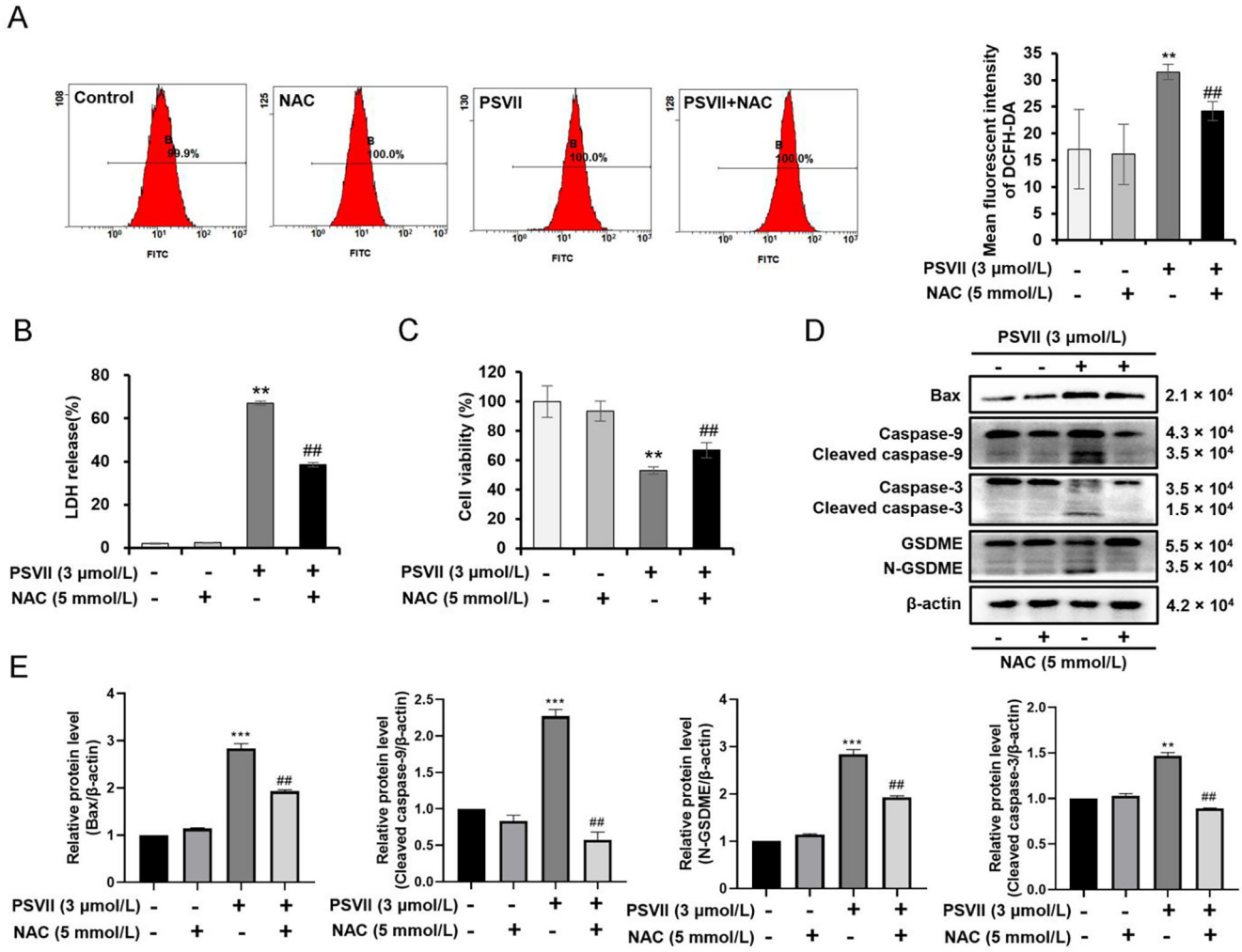

Fig. 6. PSVII triggered PDAC cell pyroptosis was facilitated by ROS/Bax signaling. (A) Intracellular ROS were measured with DCFH-DA by flow cytometry. (B–E) BxPC-3 cells were treated with PSVII in absence or presence of NAC, LDH release was measured (B), cell viability was analyzed (C), and Western blotting analysis was performed against Bax, Caspase-9, GSDME, Caspase-3 and β-actin (D–E). Mean ± SD (n = 3); $^{**}P < 0.01$, $^{***}P < 0.001$ *vs* control group; $^{\#\#}P < 0.01$ *vs* PSVII-treated group.

induced pyroptosis, LDH levels in mice serum were further detected. Compared to those in the control group, the serum LDH levels were significantly elevated in both the PSVII H treatment and gemcitabine treatment groups (Fig. 7E). Furthermore, Western blotting was used to analyze the protein levels in tumor tissues, and the results revealed that PSVII dose-dependently upregulated N-GSDME and cleaved Caspase-3 (Fig. 7F). The immunohistochemistry assessment of the tumors also revealed that both Caspase-3 (Fig. 7G) and GSDME (Fig. 7H) were upregulated in the PSVII treated group compared to the control group. Overall, these data demonstrated that PSVII suppressed the growth of PDAC tumors *in vivo via* the induction of cancer cell pyroptosis.

4. Discussion

In the present study, PSVII, an anti-cancer drug candidate isolated from the traditional Chinese herbal medicine *Paridis Rhizoma*, substantially inhibited PDAC *in vitro* and *in vivo via* the induction of pyroptosis. The underlying mechanism was also studied, and the anti-tumor activity of PSVII was shown to be related to its ability to stimulate ROS and activate the mitochondrial apoptotic pathway.

Cancer remains a major cause of death in China (Bray, Laversanne, Weiderpass, & Soerjomataram, 2021). Since 2000, both cancer cases and mortality have increased gradually in China (Tian et al., 2023; Wei et al., 2020). The incidence continues to increase for 6 of the top 10 cancers, which include pancreas (Siegel et al., 2024). Due to the lagging progress in cancer prevention and early diagnosis, most patients with PDAC are at a progressed stage at the time of clinical diagnosis and have limited opportunities for surgical treatment, so chemotherapy remains the primary solution. Therefore, new therapeutic targets and agents with high therapeutic value are imminently needed. In the present study, we showed that PSVII can inhibit the viability and migration of PDAC cells through cell viability, colony formation, Transwell migration, and wound scratch healing assays. In addition, in a xenograft tumor model of PDAC, treatment with PSVII significantly suppressed tumor growth. Combined with the findings of previous studies (Fan et al., 2015; Liu et al., 2023; Qian et al., 2020; Zhang et al., 2014), these data further prove the therapeutic potential of PSVII in cancers.

Pyroptosis is a type of PCD that has been widely studied and focused on in recent years. Initially, pyroptosis was considered Caspase-1-dependent PCD, but subsequent studies have gradually shown that Caspase-4/5/11 can also induce pyroptosis (Kayagaki

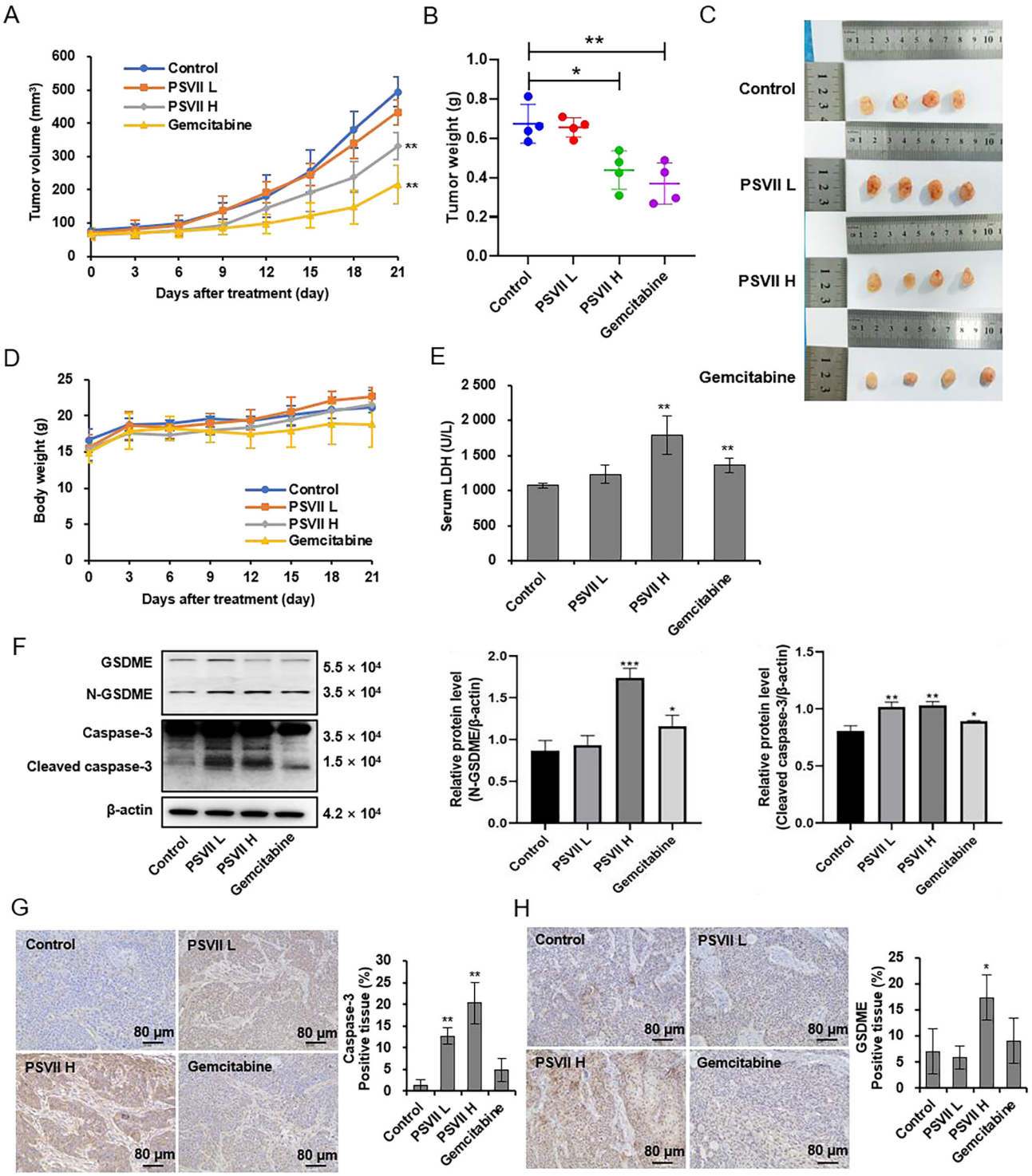

Fig. 7. PSVII suppressed tumor growth and induced PDAC cell pyroptosis *in vivo*. BxPC-3 cells were inoculated into nude mice to establish a tumor model *in vivo*, as described in the materials and methods section. Tumor-bearing mice were randomly grouped and administered NS (control), 1.25 mg/kg body weight of PSVII (PSVII L), 2.5 mg/kg body weight of PSVII (PSVII H), or 60 mg/kg body weight of gemcitabine. (A) Tumor volume was measured every three days. (B) Tumors were dissected and weighed. (C) Representative photographs of isolated tumors on day 21 post-treatment. (D) Body weights of mice were recorded during 21-day period. (E) Serum LDH levels were examined. (F) Western blotting analysis of GSDME, N-GSDME, Caspase-3, and Cleaved caspase-3 expression in tumor tissues. (G and H) Immunohistochemical analysis of Caspase-3 (G) and GSDME (H) in tumors; scale bar = 80 μm, × 100. Mean ± SD (n = 4); $^{*}P < 0.05$, $^{**}P < 0.01$, $^{***}P < 0.001$ *vs* control group.

et al., 2015; Shi et al., 2015). Recent studies have described pyroptosis as PCD executed by gasdermins, which requires cleavage by inflammatory caspases or other upstream factors (Yang, Bettadapura, Smeltzer, Zhu, & Wang, 2022; Zhou et al., 2020). At present, the mechanism by which most chemotherapeutic drugs induce PCD is induction of apoptosis, however, resistance to apoptosis results in treatment failure (Makin & Dive, 2001). Thus, drug candidates that induce pyroptosis, a non-apoptotic type of PCD, could present exciting therapeutic opportunities for overcoming the failure of chemotherapy in certain circumstances.

Previous research has shown that the anti-cancer activity of PSVII is related to its ability to suppress cell growth and trigger cell

apoptosis and autophagy (Qian et al., 2020; Xiang et al., 2022; Zhou et al., 2019). We proposed that Caspase-3/GSDME-dependent pyroptosis participates in PSVII induced PDAC cell death in this study. The features of pyroptosis, which include GSDME cleavage, LDH release, pore formation in the plasma membrane, and PI uptake enhancement, were observed in PSVII treated PDAC cells. As reported, cell membrane permeabilization and cell rupture are also features of cells undergoing necroptosis (Yan, Wan, Choksi, & Liu, 2022), thus, an inhibitor of necroptosis, necrostatin-1, was applied to determine the type of cell death triggered by PSVII. The necrostatin-1 had no obvious effect on cell viability or the induction of LDH release, revealing that necroptosis was not induced by PSVII. The GSDM family members, which are involved in pore formation, are the final executors of pyroptosis. The expression of GSDMs was confirmed in three PDAC cell lines, among which GSDMD and GSDME were found to be expressed in PDAC cells. GSDMD cleavage has also been shown to trigger pyroptosis in previous studies. However, after PSVII treatment, GSDME was cleaved significantly more than GSDMD, that was, PSVII did not evoke cleavage of GSDMD. Knockdown of GSDMD by siRNA did not affect PSVII induced cell death or LDH release, therefore, GSDMD was not involved in PSVII induced pyroptosis in PDAC cells. After PSVII intervention, the BxPC-3 cells rapidly entered the double-positive stage for Annexin V/PI staining, and siRNA-mediated knockdown of GSDME delayed this process. The number of Annexin V-positive cells increased, while the proportion of Annexin V/PI double-positive cells was reduced. Furthermore, knocking down of GSDME resulted in a significant reduction in PSVII induced LDH release, but did not rescue cell death in consequence of PSVII treatment, thus which confirmed the switch from pyroptosis to apoptosis. This study also suggested that PSVII intervention decreased the mitochondrial membrane potential, increased the protein level of Bax, and increased the cleavage of Caspase-9, Caspase-3, and GSDME, while reducing the level of Bcl-2 in BxPC-3 cells. Moreover, Z-DEVD-FMK, a specific inhibitor of Caspase-3, significantly inhibited PSVII triggered pyroptosis, downregulated the LDH release, and decreased the percentage of double-positive stage of Annexin V and PI, while increasing the proportion of Annexin V single-positive cells. Previous investigations have also illustrated that GSDME-dependent pyroptosis can be induced by activating the mitochondrial apoptotic pathway (Lu et al., 2018; Rogers et al., 2017), which was consistent with our study, and demonstrated that the activation of caspases *via* the mitochondrial apoptotic pathway was necessary for PSVII induced pyroptosis in PDAC cells. In addition, a xenograft tumor model was generated to further demonstrate the anti-PDAC effect of PSVII *in vivo*, which found that PSVII reduced the tumor burden and induced tumor cell pyroptosis in PDAC tumor models. Besides, the average body weights of mice in the PSVII-treated group remained relatively stable compared to those in the control group, while the gemcitabine group exhibited a tendency towards decreased body weights (although the difference was not statistically significant). These observations indicated PSVII treatment had no significant effects on the body weight and growth of mice, and preliminarily suggested PSVII had low toxicity in mice.

Many chemotherapeutic agents induce apoptosis in cancer cells. With the extensive use of these drugs, resistance to apoptosis plays an irreplaceable role in chemoresistance, leading to treatment failure. Therefore, patients with pancreatic cancer and other aggressive tumors, who have low survival rates, continue to struggle with the disease. On this occasion, further investigation was conducted into pyroptosis, a newly recognized type of PCD, as well as the relationship between pyroptosis and apoptosis. Preliminary investigations reveal that pyroptosis and apoptosis, two types of PCD, may reciprocally regulate each other, leading to cytotoxic inhibition (Jiang, Qi, Li, & Li, 2020). Caspase-3 and GSDME are identified as key proteins that determine the form of cell death. GSDME is considered as a crucial molecule in the transition between cell apoptosis and pyroptosis. When GSDME is highly expressed, pyroptosis is conducted in a Caspase-3-dependent manner to induce tumor cell death. However, when GSDME is expressed at low levels, cytotoxic drugs induced cell death is converted to apoptosis rather than pyroptosis (Rogers et al., 2017; Wang et al., 2017). Studies have shown that after chemotherapy, apoptosis and pyroptosis, two forms of PCD, may occur simultaneously (Lu et al., 2018; Yu et al., 2019). Our findings demonstrated that both apoptotic and pyroptotic markers can be synchronously detected in BxPC-3 cells treated with PSVII. We also believed that there is an interplay between pyroptosis and apopto-

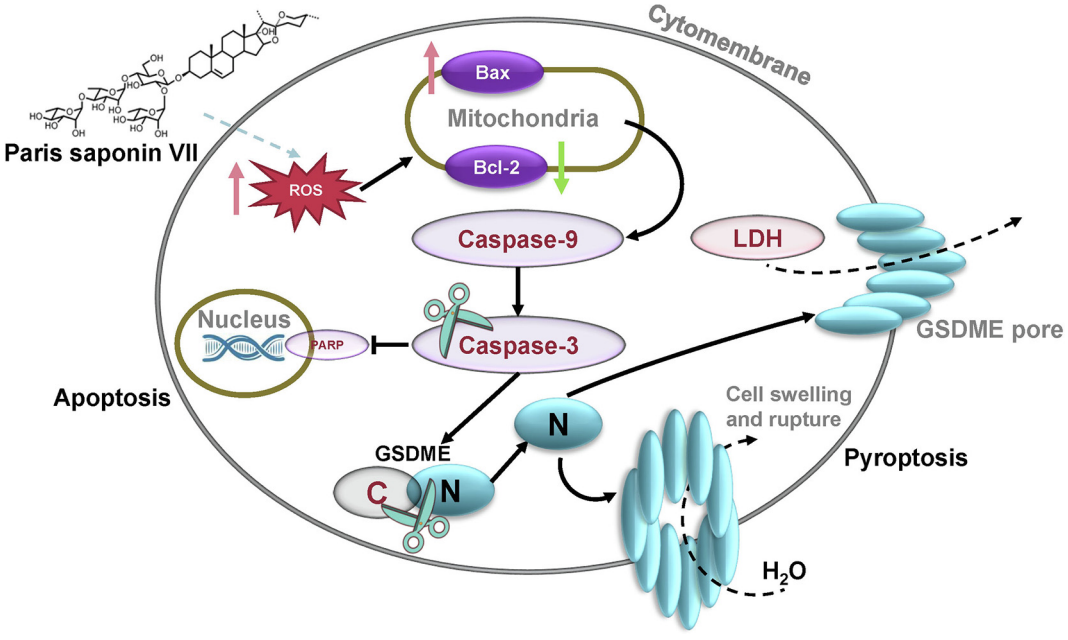

Fig. 8. A schematic summary of this study.

sis, where different intracellular Caspase-cleaved substrates are responsible for the different types of PCD. The knockdown of GSDME shifts cell death from pyroptosis to apoptosis, which may be due to PARP being cleaved by Caspase-3 in this situation, leading to increased apoptosis, and further suggesting that chemotherapy-induced pyroptosis might occur first (Fig. 8).

Previous research has indicated that, in cancer cells, PSVII triggered ROS accumulation is crucial for apoptosis (Zhang et al., 2016; Zhao et al., 2021). The excess accumulated ROS leads to the oligomerization of membrane proteins, which can recruit Bax to the mitochondrial membrane, thereby promoting the release of cytochrome *C* to activate the cleavage of Caspase-3, ultimately inducing pyroptosis by cleaving GSDME (Li et al., 2023; Zhou et al., 2018). This is consistent with our results, which show that PSVII elevates ROS production and activates Bax/Caspase-3/GSDME signaling to induce pyroptosis in PDAC cells. The ROS scavenger NAC suppressed the release of LDH and the cleavage of Caspase-9, Caspase-3, and GSDME in BxPC-3 cells, eventually reversing PSVII-induced pyroptosis.

Although many investigations have shown that pyroptosis enhances the sensitivity of tumors to chemotherapeutic drugs and reduces chemotherapy resistance, high GSDME expression may also increase side effects (Jiang et al., 2020). In addition, inflammatory cytokines are released during pyroptosis, which may lead to inflammatory carcinogenesis. Therefore, there are still many problems that need to be solved regarding the relationship between Caspase-3 and GSDME in the future.

5. Conclusion

Our current study indicates that PSVII may be a potential drug candidate for treating PDAC. PSVII induced Caspase-3/GSDME-dependent pyroptosis *via* the activation of ROS/Bax-related mitochondrial signaling (Fig. 8). Collectively, these findings provide new insights into the therapeutic action of PSVII through Caspase-3/GSDME-dependent pyroptosis, an unidentified mechanism by PSVII treatment in cancers, and which may constitute a novel strategy for combating chemotherapy resistance in PDAC.

CRediT authorship contribution statement

Xiaoying Qian: Writing – original draft, Validation, Methodology. **Yang Liu:** Writing – original draft, Validation. **Wenwen Chen:** Data curation. **Shuxian Zheng:** Data curation. **Yunyang Lu:** Conceptualization, Writing – review & editing. **Pengcheng Qiu:** Conceptualization, Writing – review & editing. **Xisong Ke:** Writing – review & editing. **Haifeng Tang:** Writing – review & editing, Funding acquisition. **Xue Zhang:** Writing – review & editing, Resources.

Declaration of competing interest

The authors declare that they have no known competing financial interests or personal relationships that could have appeared to influence the work reported in this paper..

Acknowledgments

This work was supported by the National Natural Science Foundation of China (No. 81973192).

References

Bray, F., Laversanne, M., Weiderpass, E., & Soerjomataram, I. (2021). The ever-increasing importance of cancer as a leading cause of premature death worldwide. *Cancer, 127*(16), 3029–3030.

Chen, X., He, W. T., Hu, L., Li, J., Fang, Y., Wang, X., ... Han, J. (2016). Pyroptosis is driven by non-selective gasdermin-D pore and its morphology is different from MLKL channel-mediated necroptosis. *Cell Research, 26*(9), 1007–1020.

De Dosso, S., Siebenhuner, A. R., Winder, T., Meisel, A., Fritsch, R., Astaras, C., ... Borner, M. (2021). Treatment landscape of metastatic pancreatic cancer. *Cancer Treatment Reviews, 96*, 102180.

Ding, J., Wang, K., Liu, W., She, Y., Sun, Q., Shi, J., ... Shao, F. (2016). Pore-forming activity and structural autoinhibition of the gasdermin family. *Nature, 535*(7610), 111–116.

Fan, L., Li, Y., Sun, Y., Han, J., Yue, Z., Meng, J., ... Mei, Q. (2015). Paris saponin VII inhibits the migration and invasion in human A549 lung cancer cells. *Phytotherapy Research, 29*(9), 1366–1372.

He, H., Liu, Y., Qian, X. Y., Jin, M. F., Zheng, L., & Cheng, Z. (2021). Effect and mechanism of polyphyllin VII on proliferation, migration and invasion of pancreatic cancer PANC-1 cells. *Chinese Traditional and Herbal Drugs, 52*(7), 1981–1986.

Hu, L., Chen, M., Chen, X., Zhao, C., Fang, Z., Wang, H., & Dai, H. (2020). Chemotherapy-induced pyroptosis is mediated by BAK/BAX-caspase-3-GSDME pathway and inhibited by 2-bromopalmitate. *Cell Death & Disease, 11*(4), 281.

Jiang, M., Qi, L., Li, L., & Li, Y. (2020). The caspase-3/GSDME signal pathway as a switch between apoptosis and pyroptosis in cancer. *Cell Death Discovery, 6*, 112.

Kayagaki, N., Stowe, I. B., Lee, B. L., O'Rourke, K., Anderson, K., Warming, S., ... Dixit, V. M. (2015). Caspase-11 cleaves gasdermin D for non-canonical inflammasome signalling. *Nature, 526*(7575), 666–671.

Li, Y., Zhao, R., Xiu, Z., Yang, X., Zhu, Y., Han, J., ... Li, Y. (2023). Neobavaisoflavone induces pyroptosis of liver cancer cells via Tom20 sensing the activated ROS signal. *Phytomedicine, 116*, 154869.

Liu, Y., Liu, M. Y., Bi, L. L., Tian, Y. Y., Qiu, P. C., Qian, X. Y., ... Zhang, B. L. (2023). Cytotoxic steroidal glycosides from the rhizomes of *Paris polyphylla* var. *yunnanensis*. *Phytochemistry, 207*, 113577.

Lu, H., Zhang, S., Wu, J., Chen, M., Cai, M. C., Fu, Y., ... Zhuang, G. (2018). Molecular targeted therapies elicit concurrent apoptotic and GSDME-dependent pyroptotic tumor cell death. *Clinical Cancer Research, 24*(23), 6066–6077.

Makin, G., & Dive, C. (2001). Apoptosis and cancer chemotherapy. *Trends in Cell Biology, 11*(11), S22–S26.

Miao, E. A., Rajan, J. V., & Aderem, A. (2011). Caspase-1-induced pyroptotic cell death. *Immunological Reviews, 243*(1), 206–214.

Mizrahi, J. D., Surana, R., Valle, J. W., & Shroff, R. T. (2020). Pancreatic cancer. *The Lancet, 395*(10242), 2008–2020.

Mohammad, R. M., Muqbil, I., Lowe, L., Yedjou, C., Hsu, H. Y., Lin, L. T., ... Azmi, A. S. (2015). Broad targeting of resistance to apoptosis in cancer Suppl(0). *Seminars in Cancer Biology, 35*, S78–S103.

Qian, S., Tong, S., Wu, J., Tian, L., Qi, Z., Chen, B., ... Zhang, Y. (2020). Paris saponin VII extracted from *Trillium tschonoskii* induces autophagy and apoptosis in NSCLC cells. *Journal of Ethnopharmacology, 248*, 112304.

Rogers, C., Fernandes-Alnemri, T., Mayes, L., Alnemri, D., Cingolani, G., & Alnemri, E. S. (2017). Cleavage of DFNA5 by caspase-3 during apoptosis mediates progression to secondary necrotic/pyroptotic cell death. *Nature Communications, 8*, 14128.

Shi, J., Gao, W., & Shao, F. (2017). Pyroptosis: Gasdermin-mediated programmed necrotic cell death. *Trends in Biochemical Sciences, 42*(4), 245–254.

Shi, J., Zhao, Y., Wang, K., Shi, X., Wang, Y., Huang, H., ... Shao, F. (2015). Cleavage of GSDMD by inflammatory caspases determines pyroptotic cell death. *Nature, 526*(7575), 660–665.

Siegel, R. L., Giaquinto, A. N., & Jemal, A. (2024). Cancer statistics 2024. *CA: A Cancer Journal for Clinicians, 74*(1), 12–49.

Tian, Y., Ma, B., Yu, S., Li, Y., Pei, H., Tian, S., ... Wang, Z. (2023). Clinical antitumor application and pharmacological mechanisms of Dahuang Zhechong Pill. *Chinese Herbal Medicines, 15*(2), 169–180.

Wang, Y., Gao, W., Shi, X., Ding, J., Liu, W., He, H., ... Shao, F. (2017). Chemotherapy drugs induce pyroptosis through caspase-3 cleavage of a gasdermin. *Nature, 547*(7661), 99–103.

Wei, W., Zeng, H., Zheng, R., Zhang, S., An, L., Chen, R., ... He, J. (2020). Cancer registration in China and its role in cancer prevention and control. *The Lancet Oncology, 21*(7), e342–e349.

Xiang, Y. C., Peng, P., Liu, X. W., Jin, X., Shen, J., Zhang, T., ... Liu, Y. (2022). Paris saponin VII, a Hippo pathway activator, induces autophagy and exhibits therapeutic potential against human breast cancer cells. *Acta Pharmacologica Sinica, 43*(6), 1568–1580.

Yan, J., Wan, P., Choksi, S., & Liu, Z. G. (2022). Necroptosis and tumor progression. *Trends Cancer, 8*(1), 21–27.

Yang, F., Bettadapura, S. N., Smeltzer, M. S., Zhu, H., & Wang, S. (2022). Pyroptosis and pyroptosis-inducing cancer drugs. *Acta Pharmacologica Sinica, 43*(10), 2462–2473.

Yu, J., Li, S., Qi, J., Chen, Z., Wu, Y., Guo, J., ... Zheng, J. (2019). Cleavage of GSDME by caspase-3 determines lobaplatin-induced pyroptosis in colon cancer cells. *Cell Death & Disease, 10*(3), 193.

Zhang, C. C., Li, C. G., Wang, Y. F., Xu, L. H., He, X. H., Zeng, Q. Z., ... Ouyang, D. Y. (2019). Chemotherapeutic paclitaxel and cisplatin differentially induce pyroptosis in A549 lung cancer cells via caspase-3/GSDME activation. *Apoptosis, 24*(3–4), 312–325.

Zhang, C., Jia, X., Bao, J., Chen, S., Wang, K., Zhang, Y., ... He, C. (2016). Polyphyllin VII induces apoptosis in HepG2 cells through ROS-mediated mitochondrial dysfunction and MAPK pathways. *BMC Complementary Alternative Medicine, 16*, 58.

Zhang, W., Zhang, D., Ma, X., Liu, Z., Li, F., & Wu, D. (2014). Paris saponin VII suppressed the growth of human cervical cancer Hela cells. *European Journal of Medical Research, 19*(1), 41.

Zhang, Z., Zhang, Y., Xia, S., Kong, Q., Li, S., Liu, X., ... Lieberman, J. (2020). Gasdermin E suppresses tumour growth by activating anti-tumour immunity. *Nature, 579*(7799), 415–420.

Zhao, L., Liu, Z., Deng, X., Wang, J., Sun, L., Fan, L., & Zhang, Y. (2021). Polyphyllin VII induces mitochondrial apoptosis by regulating the PP2A/AKT/DRP1 signaling axis in human ovarian cancer. *Oncology Reports, 45*(2), 513–522.

Zhou, B., Zhang, J. Y., Liu, X. S., Chen, H. Z., Ai, Y. L., Cheng, K., ... Wu, Q. (2018). Tom20 senses iron-activated ROS signaling to promote melanoma cell pyroptosis. *Cell Research, 28*(12), 1171–1185.

Zhou, H., Sun, Y., Zheng, H., Fan, L., Mei, Q., Tang, Y., ... Li, Y. (2019). Paris saponin VII extracted from *Trillium tschonoskii* suppresses proliferation and induces apoptosis of human colorectal cancer cells. *Journal of Ethnopharmacology, 239*, 111903.

Zhou, Z., He, H., Wang, K., Shi, X., Wang, Y., Su, Y., ... Shao, F. (2020). Granzyme A from cytotoxic lymphocytes cleaves GSDMB to trigger pyroptosis in target cells. *Science, 368*(6494), eaaz7548.